

# Synthesis of $\text{La}_{0.9}\text{Sr}_{0.1}\text{Al}_{0.85}\text{Mg}_{0.1}\text{Co}_{0.05}\text{O}_{2.875}$ using a polymeric method

Shuai Li<sup>a,\*</sup>, Bill Bergman<sup>a</sup>, Zhe Zhao<sup>b</sup>

<sup>a</sup> Department of Materials Science and Engineering, School of Industrial Engineering and Management, Royal Institute of Technology, SE 10044 Stockholm, Sweden

<sup>b</sup> Inorganic Chemistry, Arrhenius Laboratory, Stockholm University, SE 10691 Stockholm, Sweden

Received 18 April 2008; received in revised form 31 July 2008; accepted 5 August 2008

Available online 19 September 2008

## Abstract

Nanocrystalline  $\text{La}_{0.9}\text{Sr}_{0.1}\text{Al}_{0.85}\text{Mg}_{0.1}\text{Co}_{0.05}\text{O}_{2.875}$  (LSAMC) powders were synthesized via a polymeric method using poly(vinyl alcohol) (PVA). The effect of PVA content on the synthesized powders was studied. When the ratio of positively charged valences ( $\text{M}^{n+}$ ) to hydroxyl groups ( $-\text{OH}$ ) is 1.5:1, crystalline  $\text{LaAlO}_3$  could be obtained at such a low calcination temperature as 700 °C. While at 900 °C the ratio is of less importance, since pure  $\text{LaAlO}_3$  perovskite could be formed for all powders after calcination at 900 °C. Thermal analysis (TG/DTA) was utilized to characterize the thermal decomposition behaviour of precursor powders. The chemical structure of the calcined powder was studied by Fourier transform infrared (FTIR) spectroscopy. The powder morphology and microstructure were examined by SEM. Dense pellets with well-developed submicron microstructures could be formed after sintering at 1450 °C for 5 h. Compared with the solid-state reaction method, the sintering temperature is substantially lower for powder prepared by the PVA method. This is due to the ultrafine and highly reactive powder produced. © 2008 Elsevier Ltd. All rights reserved.

**Keywords:** Nanocrystalline; Lanthanum aluminate; Perovskite; Polymeric method

## 1. Introduction

Solid oxide fuel cells (SOFCs) offer a clean, highly efficient and environmentally friendly alternative energy solution to convert chemical energy of the fuel directly to electrical energy.<sup>1</sup> The most commonly used electrolytes in SOFCs are zirconia-based oxides, which need to be operated at high temperatures (1000 °C). The high operation temperature may lead to serious problems for sealing materials, such as thermal mismatches and reaction between interface materials. Novel oxide electrolytes, which can operate at intermediate temperatures (500–800 °C), have thus attracted intensive research interests. The perovskite structure oxides ( $\text{ABO}_3$ ) have been extensively investigated for their different allotropic structures and easy accommodation for doping cations. It was reported that the Sr- and Mg-doped  $\text{LaGaO}_3$  (LSGM) have high ionic conductivity at 800 °C over a wide range of oxygen partial pressures,  $10^{-20} < P_{\text{O}_2} < 1 \text{ atm}$ .<sup>2,3</sup> Huang et al. reported an ionic conductivity of 0.17 S/cm at 800 °C for  $\text{La}_{0.8}\text{Sr}_{0.2}\text{Ga}_{0.83}\text{Mg}_{0.17}\text{O}_{3-\delta}$

samples, which remained stable over a week-long test.<sup>4</sup> The superior electrical conductivity has made LSGM one of the most promising candidates as intermediate temperature electrolytes for SOFCs.

However, there are still problems associated with the applications of LSGM electrolytes, such as high cost of gallium, poor mechanical performance,<sup>5,6</sup> and chemical stability problems with the Ni-ceramic anode.<sup>7</sup> Therefore, replacement of Ga with the low cost Al is highly desirable. Nguyen and Dokiya reported a strengthening effect of mixing  $\text{LaAlO}_3$  into LSGM, and the chemical stability of Sr-doped  $\text{LaAlO}_3$  was also confirmed.<sup>7</sup> The obstacles for the use of  $\text{LaAlO}_3$ -based electrolytes are the low ionic conductivity and the mixed conduction mechanism at high oxygen partial pressures.<sup>8–12</sup> Nomura reported that the  $\text{La}_{0.9}\text{Sr}_{0.1}\text{AlO}_{2.95}$  has a conductivity about one order of magnitude lower than that of  $\text{La}_{0.9}\text{Sr}_{0.1}\text{GaO}_{2.95}$  at 1000 °C, and explained it by the balance between crystallographic free volume and Goldschmidt tolerance factor.<sup>8</sup> Chen also found a significantly lower conductivity of doped  $\text{LaAlO}_3$  compared with doped  $\text{LaGaO}_3$ , which is attributed to the much higher bonding strength of Al–O and thus the higher formation energy of intrinsic oxygen vacancies.<sup>13</sup> Besides, the  $\text{LaAlO}_3$ -based ceramics are p-type conductors at high oxygen

\* Corresponding author. Tel.: +46 87908354; fax: +46 8216557.  
E-mail address: [shuai@kth.se](mailto:shuai@kth.se) (S. Li).

partial pressures. Park observed that  $\text{La}_{0.9}\text{Sr}_{0.1}\text{Al}_{0.9}\text{Mg}_{0.1}\text{O}_{2.9}$  was a pure ionic conductor only at oxygen partial pressure  $P_{\text{O}_2} < 10^{-10}$  atm.<sup>9</sup> However, the  $\text{LaAlO}_3$  ceramics may become good ionic or mixed conductors with suitable dopants. With double-doping of Sr and Mg in  $\text{LaAlO}_3$  materials, the conductivity of  $\text{LaAlO}_3$  is sharply enhanced within the solubility limit.<sup>13</sup> Similar enhancement from dopants was also reported by other researchers.<sup>7,9,10</sup> Recently, Basu et al. reported that Co doping could increase the conductivity of  $\text{LaAlO}_3$ -based electrolytes. The  $\text{La}_{0.9}\text{Sr}_{0.1}\text{Al}_{0.85}\text{Mg}_{0.1}\text{Co}_{0.05}\text{O}_{2.875}$  sample showed a conductivity of  $2.4 \times 10^{-2}$  S/cm at 1000 °C compared with  $4.9 \times 10^{-3}$  S/cm for  $\text{La}_{0.9}\text{Sr}_{0.1}\text{Al}_{0.85}\text{Mg}_{0.15}\text{O}_{2.875}$ .<sup>14</sup> By adding Sr and Mg to  $\text{LaAlO}_3$ , the conductivity as well as the oxygen partial pressure range for pure ionic conduction was enhanced, e.g., from  $P_{\text{O}_2} < 10^{-13}$  atm for  $\text{LaAlO}_3$  to  $P_{\text{O}_2} < 10^{-6}$  atm for  $\text{La}_{0.8}\text{Sr}_{0.2}\text{Al}_{0.95}\text{Mg}_{0.05}\text{O}_{2.875}$ .<sup>10</sup> Therefore,  $\text{LaAlO}_3$ -based ceramics are promising oxygen ion conductors at high temperature and low  $P_{\text{O}_2}$ .

The  $\text{LaAlO}_3$ -based ceramics were primarily prepared by the conventional solid-state reaction method.<sup>7–11,13</sup> The method involves high firing temperatures and time consuming regrinding process. The synthesized powders suffer from inhomogeneous composition distribution, coarse particles, and undesired impurities. Other methods, such as glycine–nitrate method,<sup>12</sup> Pechini process,<sup>14</sup> sol–gel process<sup>15</sup> and coprecipitation,<sup>16</sup> have also been used to synthesize  $\text{LaAlO}_3$ -based ceramics. It was reported by Kriven and her colleagues that a polymeric route, using the PVA as the polymeric carrier, is an effective method to synthesize fine and homogeneously mixed oxide powders.<sup>17–19</sup> Unlike the Pechini route, which involves chelation and polymerization, the PVA method involves mainly steric entrapment of cations into the polymer network. The cations are entangled in the polymer network, which prevents precipitation, and thus ensures a homogeneous mixing at atomic level. In the present work, we report a systematic study on the synthesis of LSAMC using the PVA polymeric route. The LSAMC powder calcined in the temperature range of 250–1100 °C was characterized by XRD, TG/DTA, Fourier transform infrared (FTIR) and SEM.

## 2. Experimental

### 2.1. Materials preparation

The powders were synthesized using the following chemicals:  $\text{La}(\text{NO}_3)_3 \cdot 6\text{H}_2\text{O}$  (99.99%),  $\text{Sr}(\text{NO}_3)_2$  (99.97%),  $\text{Al}(\text{NO}_3)_3 \cdot 9\text{H}_2\text{O}$  (98%),  $\text{Mg}(\text{NO}_3)_2 \cdot 6\text{H}_2\text{O}$  (99.97%) and  $\text{Co}(\text{NO}_3)_2 \cdot 6\text{H}_2\text{O}$  (98.0–102.0%) (All of them are from Alfa Aesar, a Johnson Matthey Company). To prepare the polymeric precursor for LSAMC, stoichiometric amounts of nitrate salts were mixed with the 5 wt.% PVA ( $-(\text{CH}_2-\text{CHOH})_n-$ , molecular weight of 57,000–66,000, Alfa Aesar) solution. The nitrate salts were mixed in distilled water. This solution was then added to the PVA solution, which was made by dissolving appropriate amount of PVA into distilled water and stirring on a hot plate at 150 °C. The proportions of PVA to nitrate salts were adjusted in such way that the ratios of positively charged valences to hydroxyl groups ( $\text{M}^{n+}/-\text{OH}$ ) of PVA were 1:1, 1.5:1 and 2:1,

respectively. For example, in the case of 1.5:1 for 1 mol of LSAMC, total metal valences are 5.75 mol, and then the amount of PVA corresponding to 3.83 mol hydroxyl groups is needed. The resulting precursor solution was stirred and homogenized on a hot plate for 1 h at room temperature. The solution was then heated up to 250 °C to evaporate water while stirring. No precipitation was observed during the evaporation. Black crisp char was finally formed and dried in an oven at 200 °C overnight. The char was grounded into fine powders and calcined over a temperature range of 250–1100 °C in air for 6 h.

To break the hard agglomerates of the calcined powders, the 900 °C calcined powders was subjected to ball milling using a planetary mill for 1 h.  $\text{ZrO}_2$  balls (diameter: 5 mm) were used as the milling media, and ethanol as a solvent. The 900 °C calcined and ball milled powders were uniaxially pressed into pellets with a compaction pressure of 300 MPa. Green pellets were sintered at 1450 °C for 5 h in air with a heating rate of 5 °C/min.

### 2.2. Characterization

The phases in calcined and sintered samples were analysed using powder X-ray diffraction (XRD) (X'Pert Pro, PANalytical) with  $\text{Cu K}\alpha$  radiation (45 kV, 40 mA). Scans were taken in a  $2\theta$  range of 20–80 ° with a step size of 0.017 °. Lattice parameters were evaluated from all the diffraction peaks, by means of the UNIT-CELL program.<sup>20</sup> The average grain size of the powder is estimated using the Scherrer's formula:

$$d = \frac{0.9\lambda}{\beta \cos \theta}$$

where  $d$  is the average grain size,  $\lambda$  is the wavelength of  $\text{Cu K}\alpha$ ,  $\beta$  is the full width at half maximum intensity, and  $\theta$  is the Bragg's angle.

The pyrolysis and decomposition behaviour of the LSAMC precursor powders was analyzed using thermogravimetric analysis (TG) (TAG 24, SETARAM) and differential thermal analysis (DTA) (TG-DTA 1600, Labsys) up to 1200 °C with air flow at a heating rate of 10 °C/min.  $\text{Al}_2\text{O}_3$  powder was used as reference materials in the DTA test. To analyze the structure and chemistry of the calcined powders, FTIR (IFS 55, Bruker) was performed in a range of 400–4000  $\text{cm}^{-1}$ . Dry KBr was used to form pellets for the FTIR tests. The morphology of powders and pellets was studied by scanning electron microscope (SEM) (JSM-840, JEOL). To avoid the electrical charging, powders and pellets were Pt/Au coated. The density of as sintered pellets was measured using the Archimedes method.

## 3. Results and discussion

### 3.1. Phase analysis

The XRD patterns of LSAMC powders with different  $\text{M}^{n+}/-\text{OH}$  ratios calcined at 700 °C for 6 h are shown in Fig. 1. As indicated in Fig. 1, all the diffraction peaks are from the perovskite  $\text{LaAlO}_3$  phase (JCPDS 31-0022). A broad arc-shaped continuum could be detected in the range of 25–33 ° besides the sharp diffraction peaks from  $\text{LaAlO}_3$  perovskite in powders

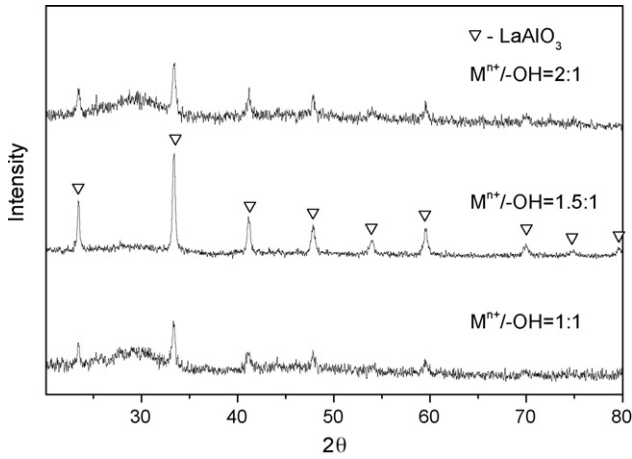


Fig. 1. XRD patterns of LSAMC powders with different  $M^{n+}/-OH$  ratios calcined at 700 °C for 6 h.

with  $M^{n+}/-OH$  ratios of 1:1 and 2:1. The arc-shaped continuum is believed to result from the amorphous phase, which remains in these two powders after calcination at 700 °C. While the LSAMC powder with 1.5:1 ratio shows a flat background, and mainly crystalline  $LaAlO_3$  is obtained at such a low calcination temperature. This implies that the powder crystallizes more easily from the amorphous precursor powder than the other two powders.

Fig. 2 shows the XRD patterns of LSAMC powders calcined at 900 °C for 6 h. Single  $LaAlO_3$  perovskite phase is obtained for all three powders after calcination at 900 °C. Since the weak broad arc-shaped continuum has disappeared, it clearly implies the complete transformation of the amorphous phases into a pure  $LaAlO_3$  perovskite. Therefore, it can be concluded that the  $M^{n+}/-OH$  ratio is of less importance when the calcination temperature is increased to 900 °C. Although the amount of PVA has no apparent effect on the phase purity of powders calcined at 900 °C, the larger amount of crystalline phase appeared in LSAMC powders with  $M^{n+}/-OH$  ratio of 1.5:1 calcined at 700 °C points out that the ratio is the optimum to produce homogeneous powders. Thus, in the following study LSAMC powders synthesized in this ratio are used.

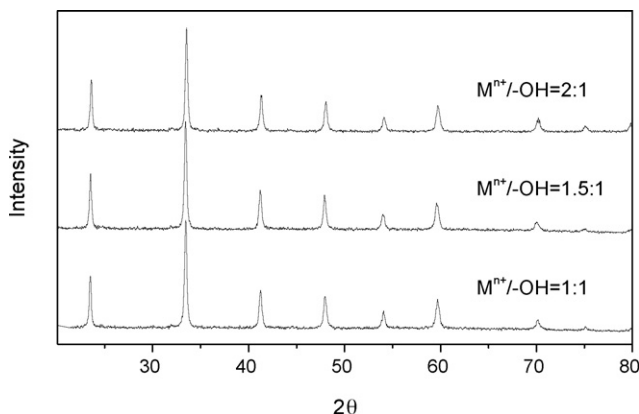


Fig. 2. XRD patterns of LSAMC powders with different  $M^{n+}/-OH$  ratios calcined at 900 °C for 6 h.

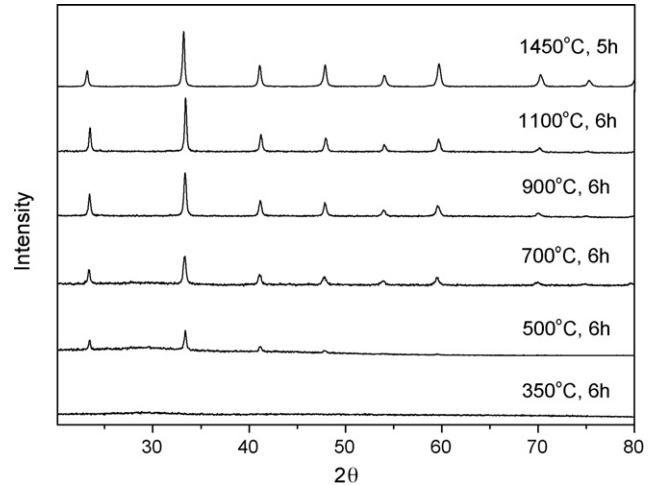


Fig. 3. XRD patterns of calcined LSAMC powders and sintered pellet.

Fig. 3 shows the XRD patterns of the LSAMC powders with  $M^{n+}/-OH$  ratio of 1.5:1 calcined at various temperatures for 6 h and pellet sintered at 1450 °C for 5 h. Fig. 3 reveals that the amorphous phase starts to crystallize around 500 °C, since the diffraction peaks from  $LaAlO_3$  perovskite phase could be first detected at this temperature. At a calcination temperature of 700 °C, it can be illustrated that mainly crystalline  $LaAlO_3$  is formed in the powder. Fully crystallized  $LaAlO_3$  perovskite phase is obtained in the powders after calcination at 900 and 1100 °C, and no amorphous phase could be found. The 1450 °C sintered pellet shows a rhombohedral  $LaAlO_3$  perovskite phase, with lattice parameters of  $a = 5.36301 \text{ \AA}$  and  $c = 13.12887 \text{ \AA}$ , which is in good agreement with the previously reported values.<sup>8,12</sup>

Furthermore, it is illustrated in Fig. 3 that no diffraction peaks from impurity phases could be detected in the XRD patterns during the firing process. It implies a perfect mixing of the constituent cations in the precursor powders prepared by the PVA process. It is believed that homogeneous mixing of cations in the precursor is of great importance to enhance purity, reactivity and homogeneity of powders.<sup>17</sup> In the PVA process, the floating metal ions are not only stabilized around the polymer by the complexation between cations and the hydroxyl groups ( $-OH$ ), but also entrapped by the polymer network.<sup>17–19</sup> The metal cations mix homogeneously at an atomic level and thus results in fine powders. Therefore, the PVA process offers the advantage of preparing homogeneous and highly reactive LSAMC powders through a much more simplified procedure. The solid-state reaction method could produce pure phase and dense  $LaAlO_3$  ceramics,<sup>7–11,13</sup> however, it suffers from tedious regrinding of powders, high sintering temperature and long firing time. As a matter of fact, synthesis of doped  $LaAlO_3$  materials using solid-state reaction method can easily be affected by the presence of impurities. Kakihana and Okubo found unreacted  $La_2O_3$  even after the powders were calcined at 1700 °C.<sup>21</sup>  $La_4Al_2MgO_{10}$  and  $LaSrAlO_4$  were observed in  $LaAl_{0.9}Mg_{0.1}O_{2.95}$  after firing at 1500 °C for 3 h.<sup>13</sup> Moreover, Nguyen et al. reported impurities such as  $SrAl_2O_4$  and (La and Al) oxides in sintered  $La_{0.9}Sr_{0.1}Al_{0.9}Mg_{0.1}O_{2.9}$  pellets.<sup>10</sup> Thus, the PVA method

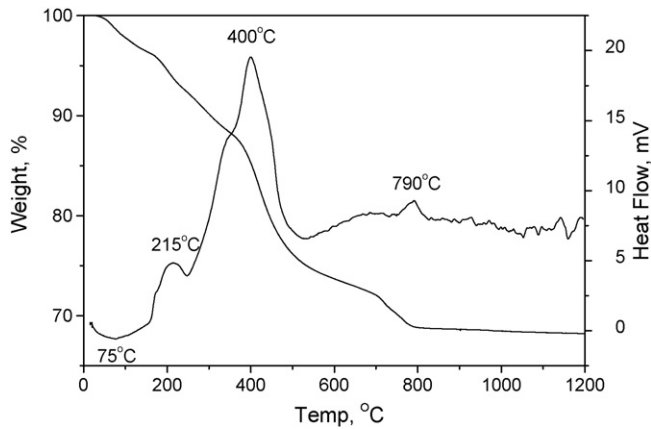


Fig. 4. TG/DTA curves of the LSAMC precursor powder at a heating rate of  $10^{\circ}\text{C}/\text{min}$ .

is quite effective at preparing phase pure LSAMC materials, compared with the conventional solid-state reaction method.

### 3.2. Thermal behaviour

Fig. 4 shows the TG/DTA curves of the LSAMC precursor powder ( $\text{M}^{n+}/\text{-OH} = 1.5:1$ ). It can be seen from the DTA curve that there are pronounced exothermic peaks around 215, 400, and  $790^{\circ}\text{C}$  and an endothermic peak around  $75^{\circ}\text{C}$ . TG analysis shows that most of the organics and nitrates decompose at temperatures  $<700^{\circ}\text{C}$ . The decomposition of LSAMC precursor powder shows three stages, which may be overlapping. In the first stage below  $160^{\circ}\text{C}$ , the weight loss (4%) is due to evaporation of free water, corresponding to the endothermic peak around  $75^{\circ}\text{C}$ . The second stage occurs over the temperature range of  $160\text{--}700^{\circ}\text{C}$ , where complex decomposition of organics and nitrates happens and corresponds to the exothermic peaks at 215 and  $400^{\circ}\text{C}$  in the DTA curve and with a thermal weight loss of 24%. The third stage shows a slight weight loss of 4.5% in temperature range of  $700\text{--}800^{\circ}\text{C}$ . This weight loss could be due to the decomposition of carbonate intermediates,<sup>18</sup> and the exothermic peak at  $790^{\circ}\text{C}$  corresponds to this process.

### 3.3. IR spectra

FTIR spectra of the LSAMC powder as a function of calcination temperature are given in Fig. 5. The broad band at  $3200\text{--}3700\text{ cm}^{-1}$  is due to the stretching vibration of the free hydroxyl group. The presence of  $\text{CO}_2$  is clearly observed in all these calcined powders. The dissolved or atmospheric  $\text{CO}_2$  is detected by the band located at  $2345\text{ cm}^{-1}$ . The presence of structural  $\text{CO}_3^{2-}$  is detected by the double bands at 1420 and  $1500\text{ cm}^{-1}$ , as well as at  $1065\text{ cm}^{-1}$ . The existence of  $\text{NO}_3^-$  is indicated by the band located at  $845\text{ cm}^{-1}$ . As illustrated by the XRD patterns in Fig. 3, there is only amorphous phase besides the crystalline perovskite  $\text{LaAlO}_3$  phase in LSAMC powders calcined below  $700^{\circ}\text{C}$ . And thus it can be concluded that the carbonate and nitrate compounds must be in an amorphous state. The lower wave number under  $690\text{ cm}^{-1}$  is due to the complex metal oxygen vibrations. As shown in Fig. 5, the hydroxyl

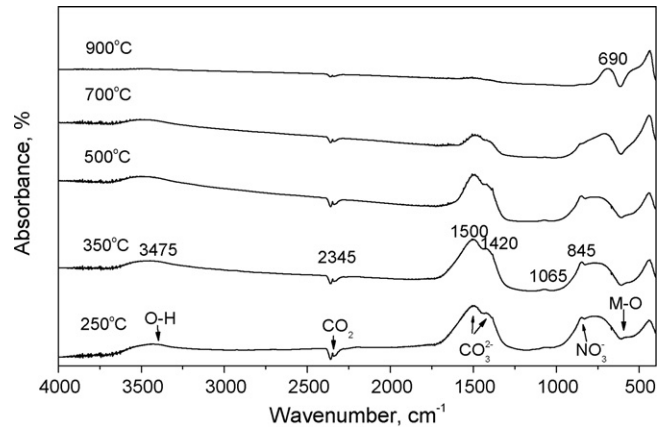


Fig. 5. FTIR spectra of LSAMC powders calcined at different temperatures.

group, carbonate and nitrate ions remain in the LSAMC powder calcined below  $700^{\circ}\text{C}$ . After calcination at  $900^{\circ}\text{C}$ , there are only  $\text{CO}_2$  and metal oxygen vibrations left in the curve, which implies that most of the organic, nitrate and carbonate intermediate compounds are completely decomposed at this stage. This result is consistent with the XRD patterns and TG analysis (see Figs. 3 and 4).

### 3.4. Powder morphology and microstructure

Fig. 6 shows the SEM morphology of  $900^{\circ}\text{C}$  calcined LSAMC powders. As discussed above, the crystallization and thermal decomposition process are complete for LSAMC powders calcined at  $900^{\circ}\text{C}$ . Ultrafine powders with primary particle sizes of  $50\text{--}100\text{ nm}$  could be demonstrated in the calcined powder from Fig. 6. The average grain size of these powders estimated from the X-ray diffraction pattern (see Fig. 3) is  $60\text{ nm}$ , in good agreement with the SEM observation.

Furthermore, Fig. 6 shows that the small particles sintered into big hard agglomerates at calcination temperature of  $900^{\circ}\text{C}$ . The presence of hard agglomerates may seriously deteriorate the density of the final sintered ceramics. Huang et al. reported a sol-gel method to prepare doped lanthanum gallate powders, and

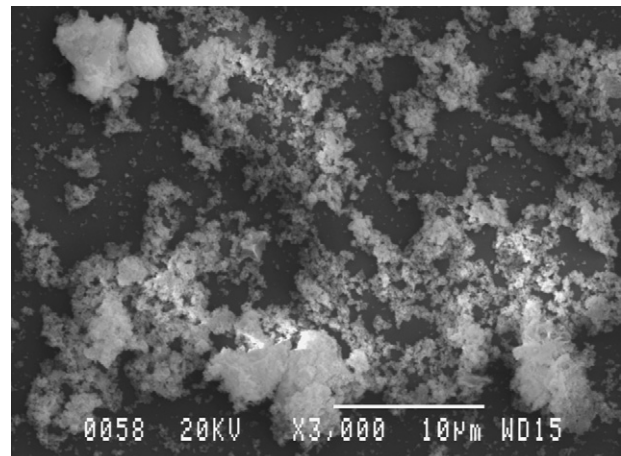


Fig. 6. SEM showing the morphology of LSAMC powders after calcination at  $900^{\circ}\text{C}$ .



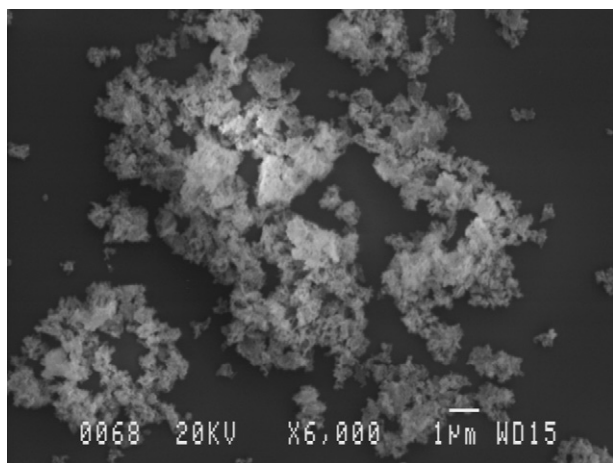


Fig. 7. SEM showing the morphology of 900 °C calcined LSAMC powders after the planetary ball milling.

found that the density of sol–gel prepared samples was generally lower than the traditional ceramic method produced ones.<sup>22</sup> A 85% relative density of lanthanum gallate pellets produced by the Pechini method was reported by Tas et al.<sup>23</sup> Although ultrafine calcined powders were prepared in both cases, the densification of the sintered pellets was apparently not satisfactory. The reason is attributed to the agglomeration of the super fine particles, and it is suggested that the milling process may be a possible way to reduce agglomeration. In a crystallization and densification study of nano-size cordierite powder by Lee, it was found that mechanical milling was needed to break up the agglomerates, and finally a nearly full densification was obtained after sintering.<sup>17</sup> Therefore, planetary ball milling was introduced to the 900 °C calcined powders in order to break up the agglomerates and enhance the densification. The SEM morphology of 900 °C calcined LSAMC powders after planetary ball milling is shown in Fig. 7. Compared with the un-milled powder (see Fig. 6), the powder shows fine and loosely packed particles instead of the hard agglomerates.

Fig. 8 illustrates the SEM microstructures of the fracture surface of a pellet after sintering at 1450 °C for 5 h. The frac-

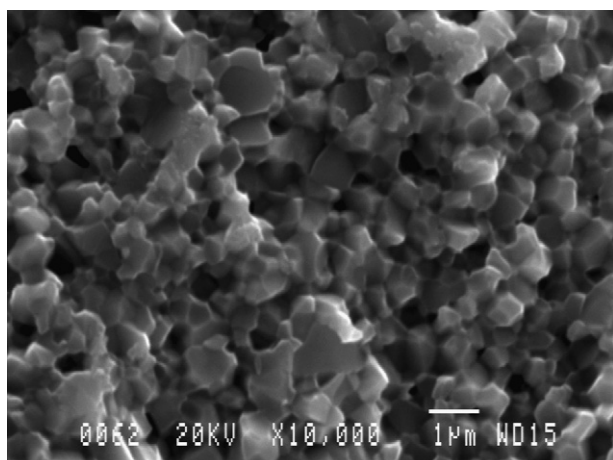


Fig. 8. Fracture surface microstructures of pellet after sintering at 1450 °C for 5 h.

ture surface morphology reveals that an intergranular fracture behaviour dominates in the LSAMC sintered pellets. Further study of the SEM microstructure illustrates that the sintered LSAMC ceramics have uniform isotropic grain morphology, and the grain size is around 0.6 µm. The density of the sintered pellet is 5.98 g/cm<sup>3</sup>, measured by the Archimedes method, and is 95% of the theoretical density. Actually, formation of single-phase perovskite is a basic issue in the processing of LaAlO<sub>3</sub>-based ceramics, but to lower the synthesis temperature using an alternative route is also rather necessary. Because the sinterability of LaAlO<sub>3</sub>-based ceramics is rather poor, the sintering temperature for the solid-state reaction method prepared powders is raised to around 1600–1700 °C. Thus, the PVA method shows advantages to prepare dense doped LaAlO<sub>3</sub> ceramics with well-developed submicron microstructures at a lower firing temperature. It has been discussed above that the PVA method can provide ultrafine and homogeneous powders with a particle size below 100 nm. Besides, the milling process introduced to the calcined powders is also found to be effective to break up the hard agglomerates evolved during calcination. Therefore, it is reasonable to conclude that this enhanced densification to get dense LSAMC ceramics at relatively lower sintering temperature is due to the fine powders and milling process.

#### 4. Conclusions

A PVA complexing method was used to synthesize LSAMC powders. It was found that mainly crystalline LaAlO<sub>3</sub> was formed for powder with 1.5:1 M<sup>n+</sup>/–OH ratio after calcination at 700 °C. The fully crystallized LaAlO<sub>3</sub> phase is obtained after calcination at 900 °C. Moreover, the XRD pattern revealed no trace of impurity phases during the heating process of LSAMC powders, which reflects the perfect mixing of metal ions in precursor powders. SEM showed that the powders calcined at 900 °C consist of fine nanocrystalline powders, although hard agglomerates are also demonstrated. The ball milling process is effective to break up the hard agglomerates and finally results in fine and loosely packed particles. The 1450 °C sintered pellet is dense and has a uniform and well-developed submicron microstructure as shown by SEM. Compared with the conventional solid-state reaction method, the PVA method is found to be effective to substantially lower the sintering temperatures. The density of the sintered pellet is 5.98 g/cm<sup>3</sup>, 95% of the theoretical density.

#### References

1. Minh, N. Q., Ceramic fuel cells. *J. Am. Ceram. Soc.*, 1993, **76**, 563–588.
2. Ishihara, T., Matsuda, H. and Takita, Y., Doped LaGaO<sub>3</sub> perovskite type oxide as a new oxide ionic conductor. *J. Am. Ceram. Soc.*, 1994, **116**, 3801–3803.
3. Huang, P. and Petric, A., Superior oxygen ion conductivity of lanthanum gallate doped with strontium and magnesium. *J. Electrochem. Soc.*, 1996, **143**, 1644–1648.
4. Huang, K., Tichy, R. S. and Goodenough, J. B., Superior perovskite oxide-ion conductor; strontium- and magnesium-doped LaGaO<sub>3</sub>: I, phase relationships and electrical properties. *J. Am. Ceram. Soc.*, 1998, **81**, 2565–2575.

5. Drennan, J., Zelizko, V., Hay, D., Ciacchi, F. T., Rajendran, S. and Badwal, S. P. S., Characterisation, conductivity and mechanical properties of the oxygen-ion conductor  $\text{La}_{0.9}\text{Sr}_{0.1}\text{Ga}_{0.8}\text{Mg}_{0.2}\text{O}_{3-x}$ . *J. Mater. Chem.*, 1997, **7**, 79–83.
6. Sammes, N. M., Keppeler, F. M., Nafe, H. and Aldinger, F., Mechanical properties of solid-state-synthesized strontium- and magnesium-doped lanthanum gallate. *J. Am. Ceram. Soc.*, 1998, **81**, 3104–3108.
7. Nguyen, T. L. and Dokiya, M., Electrical conductivity, thermal expansion and reaction of (La, Sr)(Ca, Mg) $\text{O}_3$  and (La, Sr) $\text{AlO}_3$  system. *Solid State Ionics*, 2000, **132**, 217–226.
8. Nomura, K. and Tanase, S., Electrical conduction behavior in  $(\text{La}_{0.9}\text{Sr}_{0.1})\text{M}^{\text{III}}\text{O}_{3-\delta}$  ( $\text{M}^{\text{III}} = \text{Al, Ga, Sc, In, and Lu}$ ) perovskites. *Solid State Ionics*, 1997, **98**, 229–236.
9. Park, J. Y. and Choi, G. M., Electrical conductivity of Sr and Mg doped  $\text{LaAlO}_3$ . *Solid State Ionics*, 2002, **154/155**, 535–540.
10. Nguyen, T. L., Dokiya, M., Wang, S. R., Tagawa, H. and Hashimoto, T., The effect of oxygen vacancy on the oxide ion mobility in  $\text{LaAlO}_3$ -based oxides. *Solid State Ionics*, 2000, **130**, 229–241.
11. Kilner, J. A., Barrow, P., Brook, R. J. and Norgett, M. J., Electrolytes for high-temperature fuel-cell: experimental and theoretical studies of perovskite  $\text{LaAlO}_3$ . *J. Power Sources*, 1978, **3**, 67–80.
12. Lybye, D., Poulsen, F. W. and Mogensen, M., Conductivity of A- and B-site doped  $\text{LaAlO}_3$ ,  $\text{LaGaO}_3$ ,  $\text{LaScO}_3$  and  $\text{LaInO}_3$  perovskites. *Solid State Ionics*, 2000, **128**, 91–103.
13. Chen, T. Y. and Fung, K. Z., Comparison of dissolution behavior and ionic conduction between Sr and/or Mg doped  $\text{LaGaO}_3$  and  $\text{LaAlO}_3$ . *J. Power Sources*, 2004, **132**, 1–10.
14. Basu, S., Chakraborty, A., Devi, P. S. and Maiti, H. S., Electrical conduction in nano-structured  $\text{La}_{0.9}\text{Sr}_{0.1}\text{Al}_{0.85}\text{Co}_{0.05}\text{Mg}_{0.1}\text{O}_3$  perovskite oxide. *J. Am. Ceram. Soc.*, 2005, **88**, 2110–2113.
15. Chroma, M., Pinkas, J., Pakutinskiene, I., Beganskiene, A. and Kareiva, A., Processing and characterization of sol–gel fabricated mixed metal aluminates. *Ceram. Inter.*, 2005, **31**, 1123–1130.
16. Anderson, P. S., Mather, G. C., Marques, F. M. B., Sinclair, D. C. and West, A. R., Synthesis and characterisation of  $\text{La}_{0.95}\text{Sr}_{0.05}\text{GaO}_{3-\delta}$ ,  $\text{La}_{0.95}\text{Sr}_{0.05}\text{AlO}_{3-\delta}$  and  $\text{Y}_{0.95}\text{Sr}_{0.05}\text{AlO}_{3-\delta}$ . *J. Eur. Ceram. Soc.*, 1999, **19**, 1665–1673.
17. Lee, S. J., Benson, E. A. and Kriven, W. M., Preparation of Portland cement components by poly(vinyl alcohol) solution polymerization. *J. Am. Ceram. Soc.*, 1999, **82**, 2049–2055.
18. Gulgun, M. A., Nguyen, M. H. and Kriven, W. M., Polymerized organic–inorganic synthesis of mixed oxides. *J. Am. Ceram. Soc.*, 1999, **82**, 556–560.
19. Nguyen, M. H., Lee, S. J. and Kriven, W. M., Synthesis of oxide powders by way of a polymeric steric entrapment precursor route. *J. Am. Ceram. Soc.*, 1999, **14**, 3417–3426.
20. Holland, T. J. B. and Redfern, S. A. T., UNITCELL: a nonlinear least-squares program for cell-parameter refinement implementing regression and deletion diagnostics. *J. Appl. Crystallogr.*, 1997, **30**, 84.
21. Kakahana, M. and Okubo, T., Low temperature powder synthesis of  $\text{LaAlO}_3$  through in situ polymerization route utilizing citric acid and ethylene glycol. *J. Alloys Compd.*, 1998, **266**, 129–133.
22. Huang, K. Q., Feng, M. and Goodenough, J. B., Sol–gel synthesis of a new oxide-ion conductor Sr- and Mg-doped  $\text{LaGaO}_3$  perovskite. *J. Am. Ceram. Soc.*, 1996, **79**, 1100–1104.
23. Tas, A. C., Majewski, P. J. and Aldinger, F., Chemical preparation of pure and strontium- and/or magnesium-doped lanthanum gallate powders. *J. Am. Ceram. Soc.*, 2000, **83**, 2954–2960.